

## Improvement algorithm of dynamic Allan variance and its application in analysis of FOG start-up signal

Wang Lixin, Zhu Zhanhui, Li Rui

(High-tech Institute of Xi'an, Xi'an 710025, China)

**Abstract:** The classical dynamic Allan variance(DAVAR) can describe the non-stationary of random error of fiber optical gyroscope(FOG) effectively. However, the method has defects such as poor confidence on the estimation of long-term  $\tau$ -values due to the reduced amount of data captured by the fixed length windows. Besides, the method is difficult to make a satisfactory tradeoff between dynamic tracking capabilities and variance reduction. An improved DAVAR algorithm based on kurtosis and data extension was proposed to solve the problems. Firstly, the kurtosis of data inside the windows was introduced as characterization of signal's instantaneous non-stationary, and the window length function which was utilized to truncate the signal was built by taken kurtosis as variables, the function can make window length change with the non-stationary of the signal automatically. Secondly, the random error of FOG was truncated with the function. Then the data in the windows were extended by the total variance method to improve the confidence. At last the Allan variance of extended data was computed and arranged by three-dimensional. The measured data of FOG start-up signal was analyzed with the proposed algorithm and DAVAR. The results show that the proposed algorithm is an effective way to characterize non-stationary of FOG and can also obtain a lower estimation error at long-term  $\tau$ -values.

**Key words:** fiber optical gyroscope; start-up signal; dynamic Allan variance; total variance; kurtosis

**CLC Number:** TN253    **Document code:** A    **DOI:** 10.3788/IRLA201645.0726004

## 动态 Allan 方差改进算法及其在 FOG 启动信号分析中的应用

汪立新,朱战辉,李 瑞

(西安市高科技研究所,陕西 西安 710025)

**摘 要:** 针对动态 Allan 方差运用固定长度的分析窗截取信号导致样本数据量减少,长相关时间下方差估计值置信度降低,首先,针对动态信号跟踪能力与置信度的提高不能兼顾的问题提出了一种改进算法。引入截断窗内峭度值作为表征信号短时稳定度的参数,并建立以峭度为变量的窗宽函数,该函数可以使截断窗长随着信号的平稳程度自动变化。其次,再用窗宽自适应的滑动窗分段截取陀螺随机误差,分别对每个截断窗内样本进行总方差计算以增加方差估计的自由度。最后,计算延伸后样本的 Allan 方差,并将其以三维形式排列出来。结果表明:应用该方法对光纤陀螺启动信号进行分析,该算法既能更有效地跟踪信号的非平稳变化,又能大幅降低长相关时间下方差的估计误差。

**关键词:** 光纤陀螺; 启动信号; 动态 Allan 方差; 总方差; 峭度

收稿日期:2015-11-05; 修订日期:2015-12-10

基金项目:国家自然科学基金(61503390)

作者简介:汪立新(1966-),男,教授,博士生导师,主要从事惯性技术及测试方面的研究。Email:wanglixin066@sina.cn

通讯作者:朱战辉(1978-),男,工程师,博士,主要从事惯性技术及测试、数字信号处理方面的研究。Email:zzhhit@sina.com

## 0 Introductions

The output signal of FOG changes with time due to several factors in the start-up phase, such as temperature, Shupe effect, humidity and mechanical vibrations, it demonstrates the typical non-stationary characteristic. There is a certain bias drift error in the working process of FOG, especially in the start-up phase. Characterizing and identifying the dynamic characteristics of various error sources play an important role to compensate for the drift of FOG<sup>[1]</sup>. The Allan variance is a standard quantity for the characterization of gyro, recommended by the IEEE standard. However, the Allan variance assumes the random error is stationary, and the method only can be used for analyzing statistical characteristics of FOG<sup>[2]</sup>.

Recent year, dynamic Allan variance (DAVAR) which was used to analyze non-stationary of atom clock's frequency is introduced to analyze random error of inertial sensor by some scholars<sup>[3]</sup>. Zhang Chunxi and Gu Shanshan introduced DAVAR to analyze dynamic characteristics of FOG, and the time-varying character of gyro output in vibration and temperature test is described effectively<sup>[4-5]</sup>. However, DAVAR has a poor confidence on the estimate, due to the reduced amount of data captured by the analysis windows in the computation of the Allan variance, especially at the middle-term and long-term  $\tau$ -values. Besides, the truncated window has poor flexibility resulting from the fixed length<sup>[6]</sup>. Thus, an improvement DAVAR method is proposed, as can make the length of analysis windows change with the signal stationary automatically and reduce the estimation variance of the Allan variance at the long-term  $\tau$ -values. The new method is proved validity by performing signal analysis on FOG's start-up output and simulation signal.

## 1 Dynamic Allan variance and kurtosis

The DAVAR is a sliding version of the classical

Allan variance, which can track and describe the non-stationary of signal. According to the definition of DAVAR, the original signal is truncated into data samples by a fixed length window, and the evaluation of the Allan variance in every sample is repeated, then these values are arranged in chronological order and observation interval ( $\tau$ ) order. At last the values are plotted in a single 3-D graph to represent dynamic change process of the signal.

Kurtosis is a numerical statistics which can reflect the signal distribution characteristic, and it is particularly sensitive to amplitude and standard deviation changes in the signal, it is defined as

$$K = \frac{\int_{-\infty}^{\infty} [x(t) - \bar{x}]^4 p(x) dx}{\sigma^4} \quad (1)$$

where  $x(t)$  is instantaneous amplitude;  $\bar{x}$  represents average amplitude;  $p(x)$  represents probability density;  $\sigma$  is standard deviation.

As the 4th-order central moment statistics, kurtosis can reflect the non-stationary of the signal. When the gyro is working in a stable condition, its output is close to normal distribution, and the kurtosis is relatively stable; when mutation occurs in the output of FOG, signal deviate from Gauss distribution, the kurtosis values are greater than the values in stable conditions. Thus, the kurtosis can represent the non-stationary of signal to some extent.

## 2 Ways to increase confidence of estimation

### 2.1 Total variance method

The confidence in the estimate of the Allan variance depends on the number of independent cluster time can be divided. The number is proportionate to the length of windows which are used to truncate original signal by DAVAR. However, once the length of windows is determined, the number of data inside the window will not be changed.

Fortunately, many methods were developed to

increase the confidence of limited data on the estimate of the Allan variance over the last few years, such as total variance<sup>[7]</sup>, overlapping Allan variance<sup>[8]</sup>, theoretical variance #1 and ThêoH variance<sup>[9-10]</sup>. An effective way to get around the small-sample problem is to apply a two-sided invert mirror mapping method to obtain a new virtual time series, total Allan variance is just based on this approach. The estimation of the total deviation and the Allan deviation for the same data series is shown in Fig.1. The total variance is less fluctuation than Allan variance at long-term  $\tau$ -value.

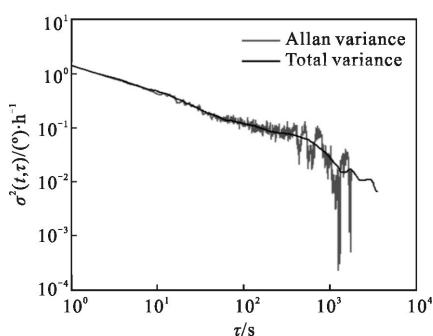


Fig.1 Log-log plot of Allan and total variance

A time-residual data  $x_i(i=1,2,\dots,N_x)$  can be extended to a new, longer virtual sequence  $x_n^*$  by mirror mapping reflection as follows:

$$\begin{cases} x_{1-j}^* = 2x_1 - x_{1+j} & (j=1, \dots, N_x-2) \\ x_i^* = x_i & (i=1, 2, \dots, N_x) \\ x_{N+j}^* = 2x_N - x_{N-j} & (j=1, \dots, N_x-2) \end{cases} \quad (2)$$

The result of this extension is a virtual data sequence  $x_n^*, 3-N_x \leq n \leq 2N_x-2$ .

### 2.2 Confidence in the estimation of total variance

Confidence, expressed as the equivalent degrees of freedom (EDF), is analysis in Reference [10] with different algorithms for computations of frequency stability at  $\tau=T/2$ . The conclusion is that the edf of ThêoH variance is larger than total Allan variance, and the total Allan variance is larger than overlapping Allan variance. But the ThêoH variance has an extremely heavy computation burden, and it is not suitable for real-time dynamic algorithm. So we choose the total variance to estimate the variance of

the data in the analysis window instead of the Allan variance. The total variance can further increase the estimation accuracy of FOG random error at long-term  $\tau$ -value than overlapping Allan variance, which has also proved in reference<sup>[8]</sup>.

## 3 Improved dynamic Allan variance

### 3.1 Establishment of adaptive window function

When we analyze the output signal of gyro, if the gyroscope is behaving in a stationary way, obviously long window can captures a larger amount of data and increase the number of samples in the computation of the Allan variance, consequently the confidence in the estimate of the DAVAR could be highly increased. Nevertheless, if long window is still used when the gyroscope is behaving in a non-stationary state, the non-stationary in the signal will not be tracked accurately and there is always an advance and delay before and after it really happens. Hence, short window will get a better choice to track fast variations in the non-stationary time series.

The instantaneous non-stationary of the signal is represented by the kurtosis value computed with data in truncation windows in the new algorithm. We use the current kurtosis values to determine subsequent truncation window length in our improved algorithm. The window length function proposed by us is

$$L(t+1) = \begin{cases} \lambda_1 & L(t) < \lambda_1 \\ L(t) - \Delta L * (K(t) - k) & \lambda_1 \leq L(t) \leq \lambda_2 \\ \lambda_2 & L(t) > \lambda_2 \end{cases} \quad (3)$$

Where  $L(t)$  is the window length of time  $t$ ;  $\lambda_1$  and  $\lambda_2$  is constant,  $\lambda_2 > \lambda_1$ , they are the upper and lower boundary for the adaptive window length. The values rest with the length of the signal to be analyzed and confidence level we expect. The threshold  $k$  is determined by the calculation of the kurtosis under stationary working state.  $\Delta L$  is the step of window length increase or decrease each time. It can be summarized that if signal is nonstationary in time  $t$ , the value of  $K(t)$  will be greater than  $k$ , and the window length  $L(t+1)$  will become shorter step by step. On the

contrary, If the signal tends to be stationary, the value of  $K(t)$  will be less than  $k$ , and the window length  $L(t+1)$  will become large gradually until to the upper boundary.

### 3.2 K-DTVAR algorithm design

The proposed algorithm is an improved DAVAR method based on kurtosis adaptive sliding window and the total variance, K-DTVAR (Kurtosis-Dynamic Total Variance) for short. We introduce the continuous-time formulation of the K-DTVAR by starting from the signal  $x(t)$  that represents the gyro signal. In Fig.2, we give a flow chart of the K-DAVAR algorithm.

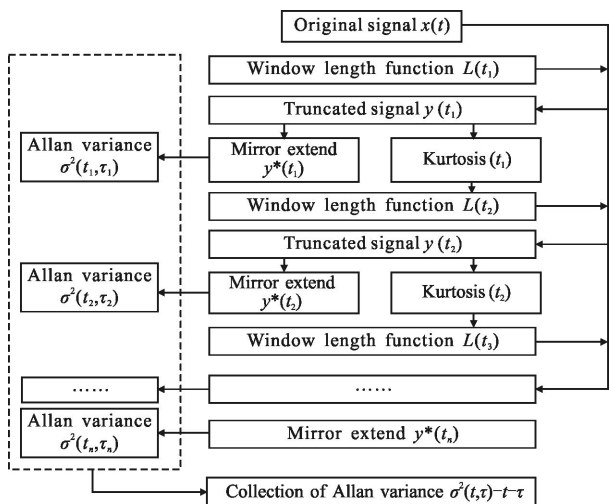


Fig.2 Flow chart of the K-DTVAR

We choose  $t_1$  as a starting point of calculate and truncate the signal  $x(t)$  with a rectangular window of length  $L(t_1)$  which center is  $t_1$ . We use support variable  $t'$  to describe the elapsing time inside the window. The interval is

$$t_1 - L(t_1)/2 \leq t' \leq t_1 + L(t_1)/2 \tag{4}$$

The truncated signal can be defined as

$$y_T(t_1, t') = y(t') P_L(t_1 - t') \tag{5}$$

$P_L(t_1 - t')$  is the rectangular window of length  $L(t_1)$ .

$$P_L(t) = \begin{cases} 1, & |t| \leq L/2 \\ 0, & \text{elsewhere} \end{cases} \tag{6}$$

Now, an extended virtual sequence  $y_T^*(t_1, t')$  can be produced by performing invert mirror method on  $y_T(t_1, t')$ , in other words, Equation(2) is applied to  $y_T(t_1, t')$ . At

the same time, the kurtosis  $K(t_1)$  of  $y_T(t_1, t')$  is computed and window length  $L(t_2)$  can be obtained by substituting in Equation (3).

We convolve  $y_T^*(t_1, t')$  with the Allan window  $h_r(t')$  to build process of increment  $\Delta(t_1, t', \tau)$ ,

$$\Delta(t_1, t', \tau) = \int_{-\infty}^{\infty} h_r(t' - t'') y_T^*(t_1, t'') dt'' \tag{7}$$

The range of the variable  $t'$  is  $t_1 - (L(t_1)/2 - \tau) \leq t' \leq t_1 + (L(t_1)/2 - \tau)$   $0 \leq \tau \leq \tau_{max}$ , the bound  $\tau_{max}$  is the maximum observation interval; it can only reach  $N\tau_0/2$  in the Allan variance estimation, but it can reach  $(N-4)\tau_0$  in the total variance. We square the increment and average in time with respect to  $t'$ .

$$\sigma_y^2(t_1, \tau) = \frac{1}{2} \langle \Delta^2(t_1, t', \tau) \rangle = \frac{1}{2(T-2\tau)} \int_{t-L(t_1)/2+\tau}^{t+L(t_1)/2-\tau} \Delta^2(t_1, t', \tau) dt' \tag{8}$$

We define the dynamic total variance as the ensemble average (expectation value) of Eq.(9).

$$\sigma_y^2(t_1, \tau) = \frac{1}{2} E[\langle \Delta^2(t_1, t', \tau) \rangle] \tag{9}$$

Some main noise coefficients  $A(t_1)_1 \dots A(t_1)_5$  can be extracted and confirmed by fitting the Allan variance curve with the least squares method.

$$\sigma^2(t_1, \tau) = \sum_{i=-2}^2 A(t_1)_i \tau^i \tag{10}$$

We choose new epoch  $t_2$  as center of window to truncate signal  $x(t)$ , then repeat the calculation process ahead, By analogy, the collection of dynamic total Allan deviation related to the different epochs  $t_n$  and the different observation intervals  $\tau$ , gives a measure of the FOG stochastic error of  $x(t)$ .

$$\sigma_y(t_1, \tau), \sigma_y(t_2, \tau) \dots \sigma_y(t_n, \tau) \tag{11}$$

## 4 Simulation results

In this section, we apply the K-DTVAR and the DAVAR to the simulation process  $x(t)$  to compare their performance in the analysis of non-stationary signal.  $x(t)$  is an uncorrelated and zero mean white Gaussian phase noise. Sampling time is 1 s, and time length is 6 000 s. Before 1 000 and after 3 000,  $\sigma=1$ , between 1 000 and 3 000,  $\sigma=2$ , the 1 000 and 3 000 is the point where the mutation occurs. Figure 3 shows the simulated

data  $x(t)$ . The data was analysis by K-DTVAR, and the result was presented in Fig.4.

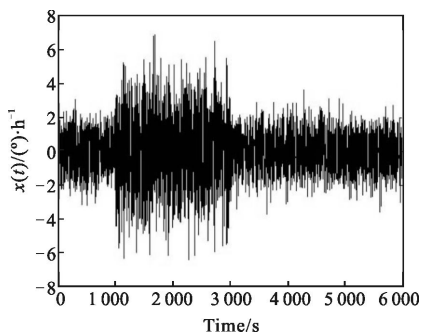


Fig.3 Dynamic white Gaussian model

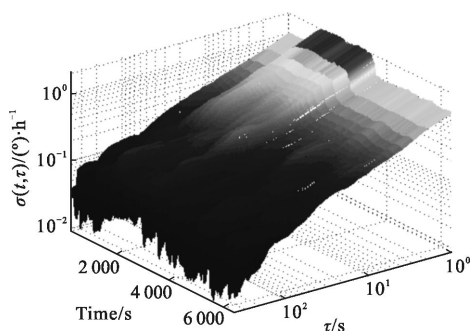


Fig.4 K-DTVAR analysis of simulation data

In Fig.5, we can observe that the length of truncation window decrease gradually when the mutation occurs and instantaneous kurtosis becomes large at 1 000 and 3 000 sampling points.

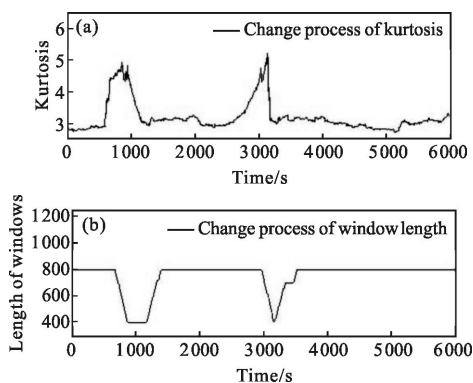


Fig.5 Change process of kurtosis and window length

The bias instability ( $B$ ) and rate random walk ( $N$ ) are two important random error sources of FOG. Dynamic tracking capabilities of K-DTVAR and DAVAR will be compared through the identification and analysis for these two noise coefficients. The

analysis results are given in Fig.6 and Fig.7, for windows of  $N=401$  samples and  $N=801$  samples by the DAVAR, for adaptive window which upper and lower boundary are 801 and 401 by the K-DTVAR.

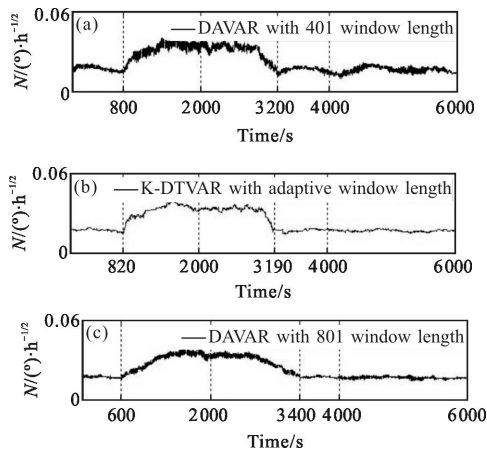


Fig.6 K-DTVAR and DAVAR analysis of rate random walk

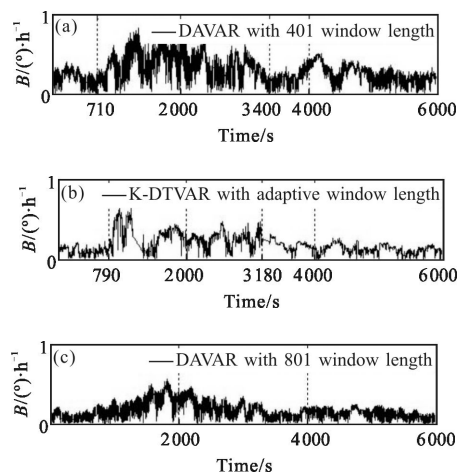


Fig.7 K-DTVAR and DAVAR analysis of bias instability

As can be seen, the K-DTVAR tracks the non-stationary more effectively. In the near 1 000 and 3 000, the transition from one region to another is very sharp, but there is instead a larger transition region from one situation to the other by DAVAR, and it is hard to point out the exact position where mutation occurred, especially for windows of  $N=801$ . Besides, the fluctuation of the noise coefficient is very large for windows of  $N=401$  samples. That also makes it hard to accurately locate the mutation points. The result is listed in Tab.1.

It seems that the dynamic tracking capability of

**Tab.1 Comparison of K-DAVAR and DAVAR in the dynamic tracking ability**

		Reference value	DAVAR 401	K-DTVAR 820	DAVAR 801
N	Start-point	1 000	800	820	600
	End-point	3 000	3 200	3 190	3 400
B	Start-point	1 000	710	790	-
	End-point	3 000	3 400	3 180	-

Notation: \*represent the point where can't be accurate positioning.

K-DTVAR is not good enough as expected. Even it is much better than the DAVAR. But it is interesting that the positioning error of K-DAVAR almost as zero if it is compensated by half of the window length (200).

### 5 Analysis for FOG start-up signal

The output of FOG is a typical non-stationary time-varying sequence in start-up phase. To further demonstrate the superiority of K-DTVAR, the K-DTVAR and the DAVAR are applied to experimental data of FOG's start-up signal respectively. The sampling period was 0.3 s and acquisition time was about 1 h. In Fig.8, the original random drift signal of FOG is shown.

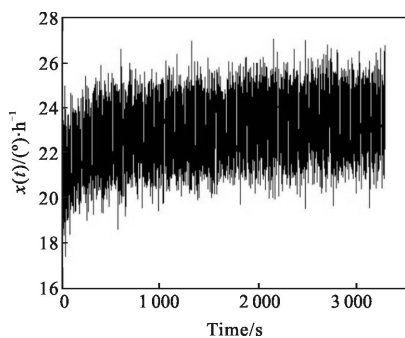


Fig.8 Start-up signal of FOG

In Fig.9 and Fig.10, we represent Allan deviation of the FOG output by K-DTVAR and DAVAR. As can be viewed, the K-DTVAR analysis figure is more clear and easy to observe. This is because the K-DTVAR makes the confidence on the estimate highly increased, especially at long-term  $\tau$ -values. On the contrary, the estimation of DAVAR tends to fluctuate

dramatically at long-term  $\tau$ -values due to a smaller amount of data inside the window.

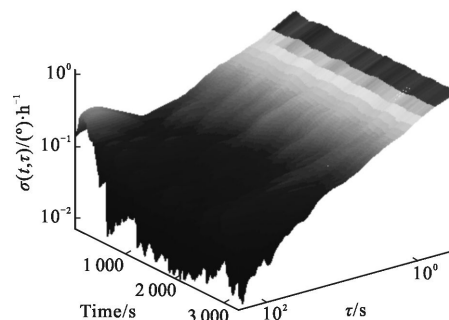


Fig.9 K-DTVAR analysis result of FOG's start-up signal

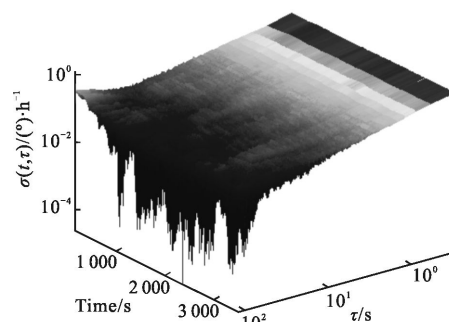


Fig.10 DAVAR analysis result of FOG's start-up signal

In addition, it can be seen by K-DTVAR that the estimate is relatively large in long-term  $\tau$ -values at the beginning of FOG's start-up phase, and which is gradually decreasing with the output of the gyro tending to be stationary, but the estimate remains the same as short-term  $\tau$ -values. However, the dynamic change is almost invisible in DAVAR analysis figure.

In Fig.11, we can observe that the length of truncation window become long gradually with the changes of kurtosis. That means we realized to track

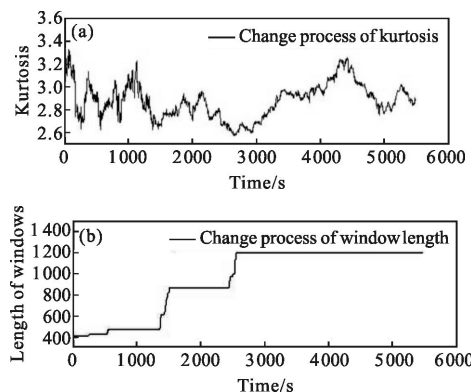


Fig.11 Change process of kurtosis, windows length and  $\tau$ -values

changes using short window in a non-stationary situation and a long window in a stationary situation.

In Fig.12, we show the change process of noise coefficients by fitting the Allan variance curve using the least squares method. It can be summarized that the A/D and D/A converters have good stability because the quantization noise ( $Q$ ) remains unchanged in FOG start-up phase. The angle random walk ( $N$ ) mainly comes from various optical components.  $N$  remaining stable means the optical components have a good stability. The bias instability ( $B$ ) is caused mainly by environmental disturbance and residual dissimilarity of FOG, representing the fluctuation of the FOG bias drift. We can judge that the output has been influenced by environment, temperature (shupe effect). The rate random walk ( $R$ ) is an important parameter for characterization FOG drift of the trend term, it changes in FOG start-up phase means the intensity of the light source or the front or rear amplifier of the detector has a one-way slow change.

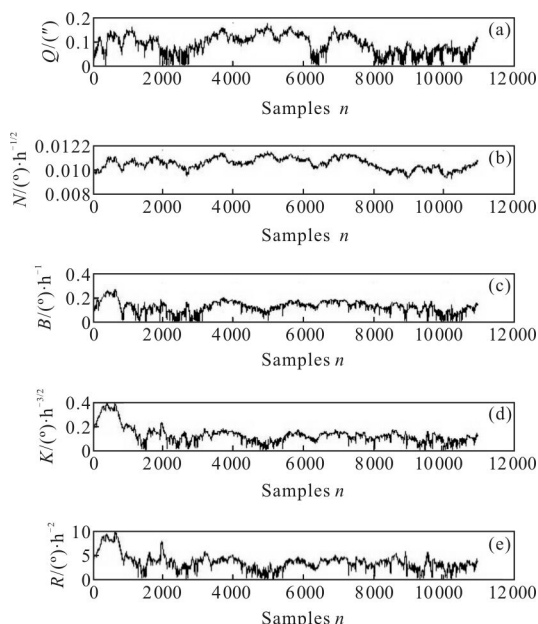


Fig.12 Change process of noise coefficients

When the FOG is behaving in a stationary way gradually, the output of FOG tends to be stable. We can take the coefficients identified by Allan variance from all of data as expected value (reference value).

And the time-varying curves of the noise coefficients by DAVAR and K-DAVAR should fluctuate on the baseline of the reference value<sup>[11]</sup>.

Here, we compare the estimating accuracy of the two algorithms. In the stationary process, that is, the 6 000 to the 9 780 points, the noise coefficients are identified by K-DTVAR and DAVAR with the same length window of  $N=1\ 201$  samples. At the same time, the estimate of the Allan variance is computed from  $N=3\ 780$  samples as the standard value of high confidence.

The change process of bias instability identified by different methods is shown in Fig.13, and the reference value 0.118 5 is the fitting result by Allan variance with 3 780 samples. Fitting results of other coefficients are given in Tab.2, values which obtained by K-DTVAR and DAVAR are average values of time-varying curves in a stationary process.

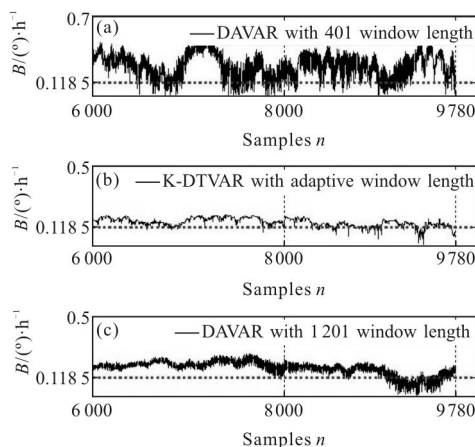


Fig.13 Change process of bias instability in stationary situation

Tab.2 Noise coefficients of FOG start-up signal

Factors	$Q/\mu\text{rad}$	$N/(\text{deg})\cdot\text{h}^{-1/2}$	$B/(\text{deg})\cdot\text{h}^{-1}$	$K/(\text{deg})\cdot\text{h}^{-3/2}$	$R/(\text{deg})\cdot\text{h}^{-2}$
Ref value	0.064 2	0.010 3	0.118 5	1.108 3	3.599 8
K-DTVAR	0.073 6	0.010 3	0.133 8	1.089 1	3.068 8
DAVAR 401	0.099 7	0.010 7	0.243 2	4.155 9	27.48 1
DAVAR1201	0.073 1	0.010 4	0.137 9	1.537 1	5.627 6

It can be seen that the noise coefficients identified by K-DTVAR are closer to the reference

value than DAVAR. With the increase of  $\tau$  value, the advantages of K-DTVAR are becoming more and more obvious.

## 6 Conclusions

For traditional DAVAR, we often have to face the choice between two opposite needs, that is, to have a good confidence or to track variation quickly, and it is difficult to have a good tradeoff with fixed length window provided by DAVAR. Therefore we propose the adaptive sliding window based on kurtosis to solve the problem successfully. Furthermore, the confidence in the estimate of the K-DAVAR is highly increased through the application of the total variance, especially at the long-term  $\tau$ -value. The proposed K-DTVAR is applied to the characterization and identification of FOG stochastic error signal. The results show: Both signal tracking capability and confidence on the estimate have greatly increased.

The proposed K-DTVAR method can be utilized to extract stochastic error coefficients of FOG in real time. Compared with the traditional compensation method based on the startup drift model which is built by historical data, the application of real-time bias instability to compensate for startup drift of FOG has more obvious advantages.

## References:

- [1] Shen Jun, Miao Lingjuan, Wu Junwei, et al. Application and compensation for startup phase of FOG based on RBF neural network [J]. *Infrared and Laser Engineering*, 2013, 42(1): 119–124. (in Chinese)
- [2] Wang Ziqiang, Zhong Mincheng, Zhou Jinhua, et al. Modeling and compensation of random drift error for optical tweezer system [J]. *Optics and Precision Engineering*, 2014, 22(6): 1403–1409. (in Chinese)
- [3] Lorenzo Galleani. Characterizing changes in the noise statistics of GNSS space clocks with the dynamic Allan variance [C]//European Signal Processing Conference, 2014: 426–430.
- [4] Zhang Chunxi, Wang Lu, Gao Shuang, et al. Dynamic Allan variance analysis for stochastic errors of fiber optic gyroscope [J]. *Infrared and Laser Engineering*, 2014, 43(9): 3081–3088. (in Chinese)
- [5] Gu Shanshan, Liu Jianye, Zeng Qinghua, et al. Dynamic Allan variance analysis method with time-variant window length based on fuzzy control[J]. *Journal of Sensors*, 2015, 2015: 1–8.
- [6] Lorenzo Galleani, Tavella P. The dynamic Allan variance[J]. *IEEE Transaction on Ultrasonics, Ferroelectrics and Frequency Control*, 2009, 56(3): 450–460.
- [7] Howe D A. The total deviation approach to long-term characterization of frequency stability[J]. *IEEE Transactions on Ultrasonic, Ferroelectrics and Frequency Control*, 2000, 47(5): 1102–1110.
- [8] Li Jintao, Fang Jiancheng. Not fully overlapping Allan variance and total variance for inertial sensor stochastic error analysis [J]. *IEEE Transactions on Instrumentation and Measurement*, 2013, 62(10): 2659–2672.
- [9] Chen Xuwei, Tang Xiaqing, Huang Xiangyuan. Investigation on random error properties of optic gyroscope based on Theoretical Variance #1 [J]. *Chinese Journal of Lasers*, 2014, 41(10): 100050031–100050038. (in Chinese)
- [10] Howe D A. ThêoH, a hybrid, high-confidence statistic that improves on the Allan deviation [J]. *Metrologia*, 2006, 43(4): 322–331.
- [11] Xu Dingjie, Miao Zhiyong, Sheng Feng, et al. Dynamic extraction MEMS gyro random error coefficients[J]. *Journal of Astronautics*, 2015: 36(2): 217–223. (in Chinese)